



Thermal analysis of new ITER FW and divertor design during VDE energy deposition

Tatyana Sizyuk^{a,*}, Ahmed Hassanein^a, Michael Ulrickson^b

^a Center for Materials Under Extreme Environment, School of Nuclear Engineering Purdue University, West Lafayette 47907, IN, USA

^b Sandia National Laboratories, Albuquerque 87185, NM, USA

HIGHLIGHTS

- We studied FW subjected to VDE heat fluxes with various steady-state conditions.
- We calculated melting and vaporization thickness of Be surface during VDE before TQ.
- We studied possible potential damage to PFC for VDEs with high energy loads.

ARTICLE INFO

Article history:

Received 18 July 2012

Received in revised form 5 December 2012

Accepted 27 January 2013

Available online 17 February 2013

Keywords:

ITER
Plasma-facing component
VDE
Coolant channel
Heat load
HEIGHTS

ABSTRACT

Further developments and investigations in the area of fusion energy devices require extensive and comprehensive computer simulations with great precision to evaluate reactor components behavior during normal and transient events. In this work we performed detailed study of the first wall (FW) subjected to high heat flux during a vertical displacement event (VDE) with various initial steady-state conditions and heat flux histories for the transient plasma energy deposition. We calculated the spatial temperature profile through out the entire module and the maximum surface temperature, as well as melting and vaporization thickness of Be surface during VDE and just before thermal quench (TQ). We further studied possible potential damage to plasma facing components (PFC) and structural materials for VDEs with higher energy loads than currently estimated.

© 2013 Elsevier B.V. All rights reserved.

1. Introduction

PFC in fusion energy reactors will be subjected to intense particle and energy loads with various intensities and time durations during normal operation and transient events that can result in several adverse effects on components and reactor operation. Interconnection of events and after-effects through plasma facing materials (PFM) erosion, eroded material transport and deposition, material properties changes due to deposited layers, structural components heating, deformation and melting, and overall performance of core plasma should be studied in detail to predict, mitigate, and possibly eliminate severe transient events during reactor operation.

The difference in scenarios and consequences of events determines the required methods and models in computer simulations

with different physical processes involved. The degree of the damage to plasma facing and structural components depends on the detailed physics of the disrupting plasma, the physics of plasma/material interactions, and the design configuration of PFC [1]. Plasma instabilities such as disruptions and ELMs, because of their short durations, will mainly cause surface damage to PFM that includes high erosion losses from vaporization, spallation, and melt-layer erosion. These events can also affect the nearby components through the distribution of eroded particles and radiation energy. Hence, correct simulation of short intense energy loads requires integration of various modeling processes into realistic reactor geometry to predict the direct heat fluxes on the divertor as well as the secondary radiation fluxes to nearby components. Accurate simulation should be self-consistent including detailed description of disrupting plasma particles interaction with solid and plasma matter; magnetohydrodynamic (MHD) of plasma evolution taking into account magnetic field diffusion; heat conduction and vaporization for tokamak PFCs; heat conduction for vapor, vapor and plasma ionization, atomic physics, and detail photon radiation transport [2].

* Corresponding author at: Purdue University, 400 Central Drive, West Lafayette, IN 47907-2017, USA. Tel.: +1 765 494 4262; fax: +1 765 496 2233.

E-mail address: tsizyuk@purdue.edu (T. Sizyuk).

Transient events, such as VDE with long time energy deposition and runaway electrons (RE) with deep penetration inside modules, can cause serious structural damage due to the high heat flux values at the components interfaces and coolant channels and possibly causing materials melting, detachment at interface, and burnout of coolant tubes. Simulation of these events requires detail geometrical consideration of PFC structure, coolant design, and parameters. For example, RE with higher energies, possible at disruptions in the ITER reactor [3], will cause increase of temperature in Cu heat sink up to melting point [4]. Structural design and material used for the coolant tube can be very important in this case as well as to mitigate their effects.

Thermal energy of the plasma during VDE is expected to be lost at the contact point. The area of strong wall contact with the plasma will absorb considerable fraction of the total plasma energy that can cause melting and vaporization of the PFC. Complex scenarios of VDEs [5] will result in increasing heat fluxes at the contact point during extended period of time before the TQ starts with intensive heat fluxes [6]. While initial temperature distribution in PFC is not very important for modeling of disruptions and ELMs, influence of the steady-state conditions and coolant parameters on melting, vaporization, and heat transfer to the coolant during VDE can be significant. At the same time, energy load during TQ is comparable with intensity and time of giant ELM [7] and modeling of such events requires consideration of processes at the surface of PFM as well as processes above the surface. During intense and fast power deposition (<10 ms) on target materials, a vapor cloud from the target debris may form above the bombarded surface. This shielding vapor layer, if well confined, will significantly reduce the net energy flux to the originally exposed target surface to only a few percent of its initial incident value; thereby substantially reducing the net vaporization rate [8]. In this case, significant part of the incident plasma energy is reradiated to nearby surfaces and little energy is conducted away from the surface to the bulk structure.

Thus, modeling of VDE with accurate prediction of consequences of this event requires considering steady-state conditions, such as normal operating heat flux and coolant parameters, simulation of energy load and distribution inside the module before TQ and integrated modeling of plasma/wall interaction, plasma motion, vapor shielding and radiation during TQ.

2. Modeling of VDE typical scenarios with ITER FW design

Critical analysis of PFCs response due to VDE energy loads was previously done using comprehensive simulations with our A*THERMAL-S and HEIGHTS 3D packages [8–10]. This analysis was preceded by the extensive study of models for vaporization, vapor shielding effect [11], heat transfer to the water coolant and critical heat flux values [10]. Our models and computer codes were tested and benchmarked against several known laboratory data for VDE relevant heat fluxes and time durations and showed excellent agreement in the simulation of both coating material erosion and melt layer thicknesses for VDE transient conditions and structural material response of copper mockup for steady-state condition as well as for loss-of-flow accident [12] and CHF criteria in smooth and swirl tubes [13].

Thermal response of ITER-like design modules to plasma VDE was studied in detail. Results of plasma energy transient deposition of 60 MJ/m² showed that Be coating significantly reduces the flow of incident plasma energy to copper structure and prevents copper melting. This is simply because of the large fraction of the incident energy removed due to extensive Be vaporization. Tungsten coating removes less plasma energy by surface vaporization and, therefore only thicker W layers allow reducing the heat flux intensity to sink material to ensure safe operation of copper and coolant channels [8,10].

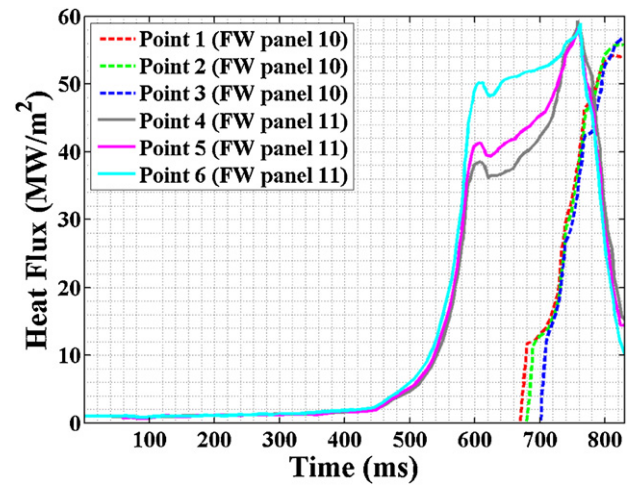


Fig. 1. Heat loads for six selected points on FW 10 and FW 11.

In this work we considered recent design of ITER FW and time-dependent heat flux to wall due to VDE. We studied the thermal response of Be surfaces during upward VDE using time histories of the thermal flux, which were calculated by VDE dynamic heat load analyses [6]. These heat flux histories, shown in Fig. 1, represent energy deposition at the locations of maximum heat load on modules 10 and 11 of ITER FW during VDE before TQ.

Modules 10 and 11 are designed for the “normal” heat flux level at steady state such as 1–2 MW/m² [14]. We considered two different design configurations of normal heat flux (NHF) panels specific to different FW locations and exposed to different heat fluxes at steady state. The FW panel 10 consists of fingers which are assumed made up of Be armor on CuCrZr heat sink with stainless steel (SS) tube of 10 mm and 12 mm inner and outer diameters respectively for water coolant. The maximum value of the peak heat flux at steady state to this panel is assumed 1 MW/m². The FW panel 11 consisting of Be armor on a CuCrZr heat sink with coolant channel of 12 mm without SS pipe is designed for a maximum heat load of 2 MW/m² at steady state. The overall configuration of ITER blanket system with poloidal cross-section and modules poloidal locations are given elsewhere [14]. The panels of rows 10 and 11 are expected to receive highest heat loads during upward VDE [6].

We simulated the effects of the high VDE heat loads with these initial conditions to predict maximum temperatures of the Be surface and at the Be/Cu interface, as well as the 3D distribution of temperature in the entire module. Additionally, we considered two thicknesses of the Be armor, i.e., 8 and 10 mm, in order to predict the impact of high heat loads on the temperature distribution inside the module as a function of Be allowable coating thickness.

Since spatial distribution of heat flux intensities on the wall surface, showed by the dynamic analysis, have non-uniform character and it will involve wide area on the FW panel, we approximated the energy deposition to the surface in HEIGHTS simulation package assuming Gaussian profile. Heat flux intensity distribution along finger with Gaussian profile of 40 cm FWHM was used in the present simulations.

3. Influence of steady-state conditions on PFC response due to VDE energies

Initially we exposed the FW 10 panel (with SS tube) to 1 MW/m² at steady state, and exposed the FW 11 panel (without SS tube) to 2 MW/m². The inlet water temperature, velocity, and pressure for both models were 115 °C, 10 m/s, and 3.6 MPa respectively. We assumed the Be armor thickness to be 8 mm.

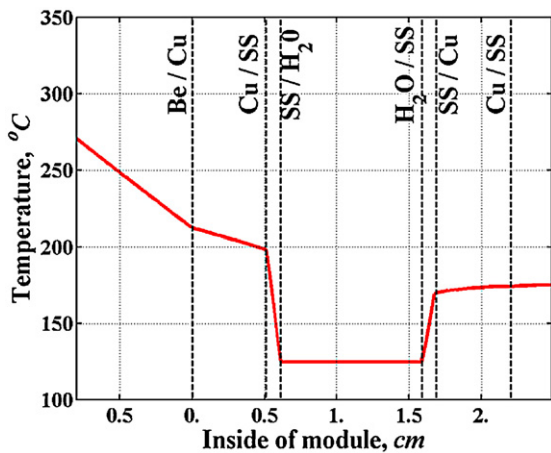


Fig. 2. Steady-state temperature distribution inside the module with 8 mm Be armor and with SS tube, 1 MW/m² steady-state heat flux (inlet water temperature of 115 °C).

The initial distribution of the temperature inside the module for the two designs is shown in Figs. 2 and 3. Despite the lower steady-state heat loads on FW 10 and the resulting lower Be surface temperature (270 °C for FW 10 and 320 °C for FW 11), the temperature values in the Cu heat sink were higher for FW 10 by ~20 °C. The low thermal conductivity of SS reduced heat conduction to the inner wall of coolant tube which resulted in reduced heat transfer to the water coolant and therefore, higher heat distribution around the tube. The increase in bulk water temperature at the outlet was 10 °C for panel 10 and 14 °C for panel 11.

Based on the dynamic analysis, contact point on FW 11 can receive ~50% of cumulated VDE energy for this location before TQ, while FW 10 can be subjected to as much as ~20% of cumulated energy before TQ. We applied VDE heat fluxes shown in Fig. 1 after the corresponding steady state fluxes for panel 10 and 11.

Figs. 4–6 show the temperature distribution in panel 11 with 8 mm Be coating: at the peak intensity of heat flux, temperature values in the Cu part of the module after the VDE high-energy deposition and steady state of 2 MW/m², and details of Cu heating in the area of the coolant wall. The maximum temperature increase on the Cu surface due to VDE was 100 degrees. We assumed for the calculation of heat transfer to the water 3.6 MPa pressure and 10 m/s velocity. These parameters allowed possible high heat sink to the

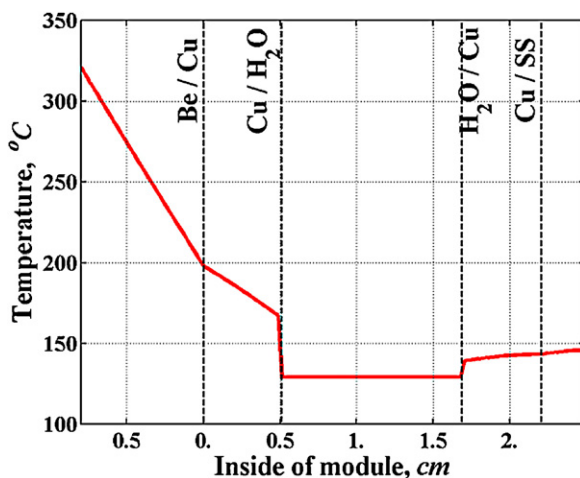


Fig. 3. Steady-state temperature distribution inside the module with 8 mm Be armor and without SS tube, 2 MW/m² steady-state heat flux (inlet water temperature of 115 °C).

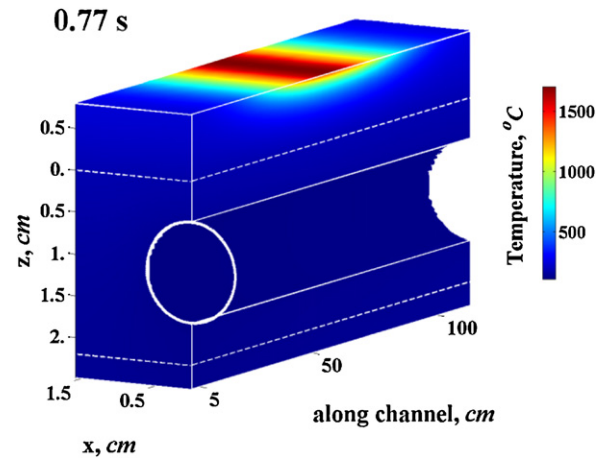


Fig. 4. Temperature distribution in panel 11 at the peak of heat load before TQ.

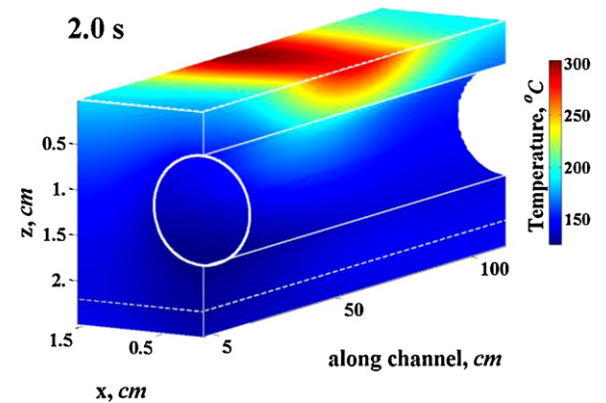


Fig. 5. Temperature distribution in copper sink of panel 11 due to VDE heat load (2 MW/m² was used for steady-state heat flux).

coolant, e.g., 5.4 MW/m² from the wall with temperature of 200 °C to the water with bulk temperature of 124 °C.

The corresponding Be surface temperatures for the considered time histories are shown in Figs. 7 and 8. Beryllium melting was not developed on the surface of FW 10 before the TQ heat loads. Melt layer thickness on FW 11 reached a maximum of 0.19 mm (Fig. 9). A few microns of Be (~3 μm) could be evaporated as a result of the high heat flux deposition before TQ.

In the next set of calculations, we analyzed the effect of the inlet water coolant parameters on Be melting using a 115 °C and 70 °C

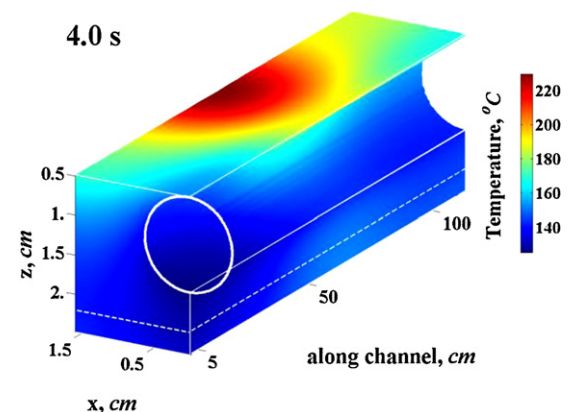


Fig. 6. Temperature distribution on coolant wall of panel 11 due to VDE heat load (2 MW/m² was used for steady-state heat flux).

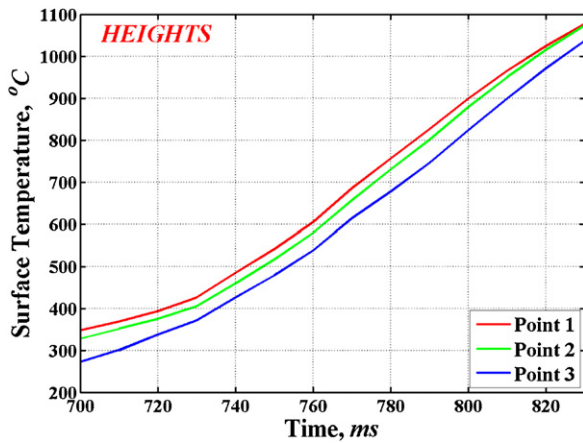


Fig. 7. Be surface temperature at points 1, 2, and 3 on FW 10, exposed to VDE heat flux before TQ.

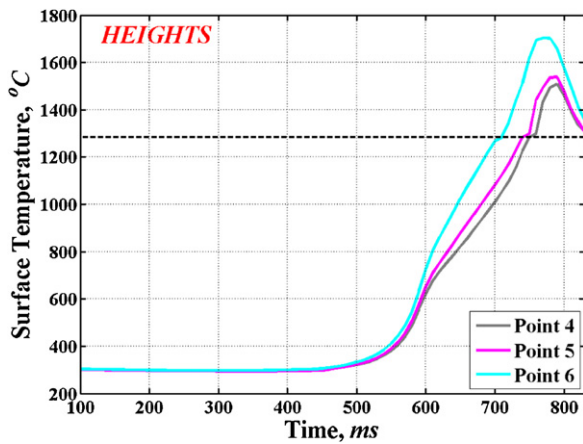


Fig. 8. Be surface temperature at points 4, 5, and 6 on FW 11, exposed to VDE heat flux before TQ.

inlet water temperature and 3 MPa pressure. Lower inlet water temperature reduced the maximum Be surface temperature by about 75 °C during VDE heat flux and the melting thickness was reduced by ~10% at the highest heat flux (point 6) of FW 11 (Fig. 10).

The effect of Be coating thickness on the surface temperature in Cu sink for two Be layer thicknesses are presented in Fig. 11. Time

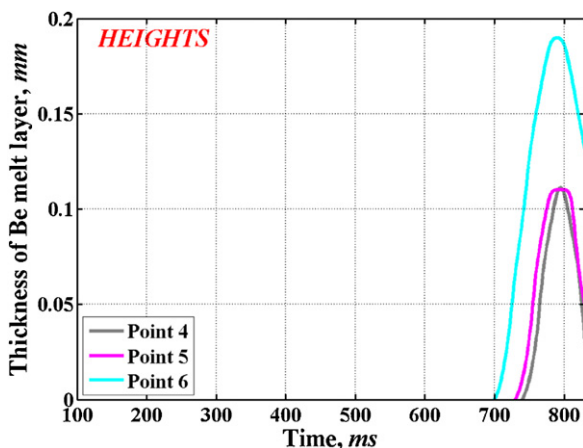


Fig. 9. Be surface melting at points 4, 5, and 6 on FW 11, exposed to VDE heat flux before TQ.

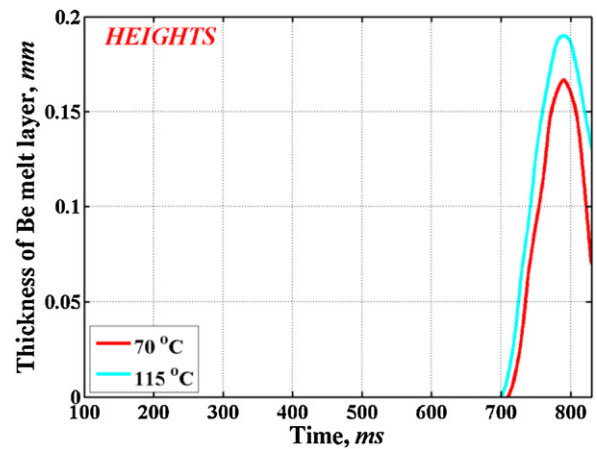


Fig. 10. Influence of inlet water temperature in coolant on Be melting thickness at highest heat load on FW 11.

evolutions of the Cu surface from the start of the VDE are shown for copper at the Be/Cu interface.

For the considered design without SS tube and the steady state conditions of 2 MW/m² before and after high heat loads to FW 11, the difference in the maximum temperature values for the two models is about 25 °C and the temperature increase in direction from the tube to the center of NHF finger is about 20 °C for Be thickness 8 mm and 16 °C for Be layer of 10 mm.

4. VDE scenarios and possible PFC damage

The ratio of the energy deposited before TQ and during TQ can be one of important characteristics of overall damage caused by plasma impact during VDE. This ratio determines the part of plasma energy transmitted inside the module, energy removed by the vaporization, and energy redistribution by the vapor shielding and resulting radiation from the developed plasma plume.

The high heat flux intensity during VDEs and their duration as well as the area involved in the interaction can significantly influence not only surface of PFC but also structural components and even coolant channels. Therefore, various possible scenarios of plasma impact during VDEs should be carefully predicted and accurately evaluated.

For example, the divertor baffle in current ITER design consists of W monoblocks with 8 mm thickness above the CuCrZr smooth tube and thin Cu interlayer [15]. Intense heat fluxes during downward

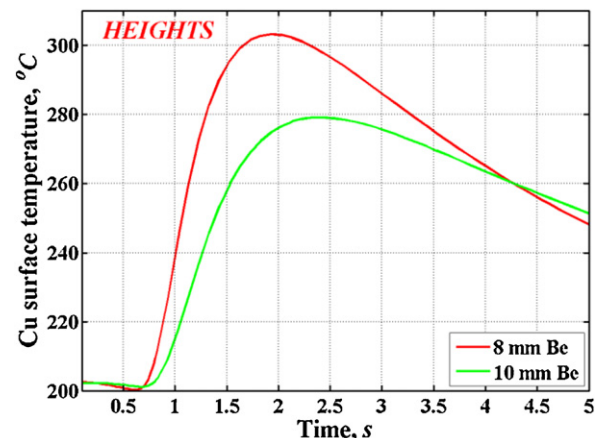


Fig. 11. Cu temperature at Be/Cu interface after VDE heat flux deposition.

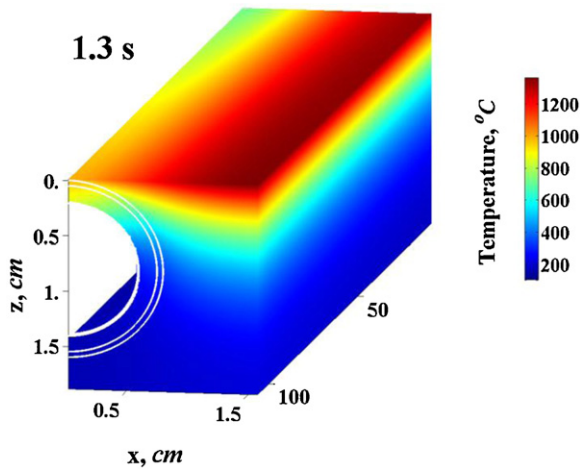


Fig. 12. Temperature distribution in lower part of W monoblock and Cu tube wall and interlayer after VDE heat flux deposition and followed 5 MW/m² steady state heat fluxes.

VDEs can impact surfaces in the divertor area [16]. Our previous simulations of high-energy load to PFC with tungsten armor showed low protection of tungsten coating with thicknesses up to 15 mm [10]. This is due to the low vaporization rate of tungsten that results in higher energy transmitted inside the module that can cause extensive melting of the copper structure. Additional effect that influence the CHF such as water coolant parameters including inlet temperature, pressure, velocity, and length of tube, should be taken into account. Fig. 12 illustrates the level of structural damage that can occur due to VDEs relevant high-energy load of 60 MJ/m² during 0.5 s, on the divertor baffle. We considered in this case the recent design of W monoblocks, highest predicted steady state fluxes in this area of 5 MW/m², and 10 m/s velocity, 3 MPa pressure, and 70 °C inlet temperature for the water in coolant channel. Fig. 12 shows higher temperatures in tungsten on the border of monoblock and temperature increase in the upper part of Cu heat sink at the end of tube due to the reduced heat transfer to the coolant when CHF was exceeded [10]. This will result in severe melting of Cu tube wall and burnout of the coolant channels.

5. Conclusion

We calculated, using our HEIGHTS simulation package, details of the thermal response and the erosion damage of PFC due to upward VDE energy loads using time histories of heat fluxes calculated from 3D dynamic analysis. Taking into account these scenarios of VDE energy loads, the recent design of NHF panels and predicted steady-state heat fluxes to these panels, the maximum melt layer developed before TQ will not exceed 0.2 mm and only a few microns of Be surface can be evaporated as a result of the high heat flux deposition before TQ.

Due to complex processes involved in the modeling of plasma material interactions during intense TQ heat fluxes following VDEs, more comprehensive HEIGHTS integrated simulations are required for the precise analysis of possible PFC damage and lifetime including integrated modeling of plasma/wall interaction, plasma MHD motion, vapor shielding, and photon radiation and their transport.

Acknowledgment

This work was partially supported by Sandia National Labs.

References

- [1] A. Hassanein, Fusion Engineering and Design 60 (2002) 527.
- [2] V. Sizyuk, A. Hassanein, Nuclear Fusion 50 (2010) 115004.
- [3] T.C. Hender, et al., Nuclear Fusion 47 (2007) S128–S202.
- [4] V. Sizyuk, A. Hassanein, Nuclear Fusion 49 (2009) 095003.
- [5] M. Sugihara, et al., Nuclear Fusion 47 (2007) 337–352.
- [6] R. Mitteau, et al., Physica Scripta T145 (2011) 014081.
- [7] A. Hassanein, I. Konkashbaev, Journal of Nuclear Materials 313–316 (2003) 664–669.
- [8] A. Hassanein, Fusion Technology 30 (1996) 713.
- [9] A. Hassanein, T. Sizyuk, M. Ulrickson, Fusion Engineering & Design 83 (2008) 1020.
- [10] A. Hassanein, T. Sizyuk, Nuclear Fusion 48 (2008) 115008.
- [11] A. Hassanein, G.L. Kulcinski, W.G. Wolfer, Nuclear Engineering and Design/Fusion 1 (1984) 307.
- [12] T.D. Marshall, J.M. McDonald, L.C. Cadwallader, D. Steiner, Fusion Technology 37 (2000) 38.
- [13] A.R. Raffray, et al., Fusion Engineering & Design 45 (1999) 377.
- [14] M. Merola, et al., Fusion Engineering & Design 85 (2010) 2312.
- [15] R.A. Pitts, et al., Journal of Nuclear Materials 415 (2011) S957–S964.
- [16] A.R. Raffray, et al., Fusion Engineering & Design 85 (2010) 93–108.